Adaptive Interval Type-2 Fuzzy Output Feedback Control Based on Nonlinear High Gain Observer for Flexible Air-breathing Hypersonic Vehicles

Xinlong Tao[1,2], Jianqiang Yi[1,2], Ruyi Yuan[1,2], and Zhen Liu[1,2]

1. Institute of Automation, Chinese Academy of Sciences, Beijing 100190, China
E-mail: {taoxinlong2014, jianqiang.yi, ruyi.yuan, liuzhen}@ia.ac.cn

2. University of Chinese Academy of Sciences, Beijing 100049, China

Abstract: In this paper, an adaptive interval type-2 fuzzy output feedback control (AIT2-FOFC) scheme is developed for flexible air-breathing hypersonic vehicles (FAHVs) in the presence of unknown flexible dynamics and parameter uncertainties. After calculating the derivatives of the velocity and altitude repeatedly, a state feedback dynamic inversion controller is formulated as the basic nominal controller. Then, an adaptive interval type-2 fuzzy logic system (AIT2-FLS) is constructed to approximate the unknown uncertainties in the FAHV longitudinal model. Furthermore, a nonlinear high gain observer is designed to estimate the high order derivatives of the velocity tracking error and altitude tracking error which are unavailable in practice. Based on the separation principle, the overall AIT2-FOFC scheme is finally obtained through combining the state feedback controller and the nonlinear high gain observer. Simulation at last demonstrates the effectiveness of our proposed control scheme.

Key Words: Flexible Air-breathing Hypersonic Vehicle, Output Feedback Control, Adaptive Interval Type-2 Fuzzy Logic System, Nonlinear High Gain Observer

1 INTRODUCTION

Since hypersonic vehicles are intended to become a more reliable and cost efficient way to access space, investigations have raised various interests all over the world. Recently, the flexible air-breathing hypersonic vehicle (FAHV) model was explored by Bolender and Doman [1]. This model focuses on the flexible dynamics of the vehicles, which may severely affect the flight safety. Besides, due to the complex design and severe flight conditions, FAHVs are sensitive to changes in the flight conditions as well as the aerodynamic parameters [2]. As a result, the control system design for FAHVs becomes a real challenge.

Recently, several control strategies based on feedback linearization technique have been proposed for hypersonic vehicles. Xu et al. developed an adaptive sliding mode controller based on an input-output linearized longitudinal model [2]. Pu et al. proposed an advanced inversion control for hypersonic vehicles based on PSO and arranged transient process [3]. Although feedback linearization technique is an efficient way for nonlinear control system design, high order derivatives of the outputs are usually hard to obtain in real applications, which few papers have taken into consideration. Li et al. employed linear high gain observer to estimate the auxiliary error signals of the hypersonic vehicles [4]. He et al. applied linear high gain observer to formulate an adaptive output feedback fault-tolerant control system [5]. However, they did not consider the side effects of the flexible dynamics.

This work is supported by NNSFC No. 61421004, 61403381, 61603384, and NDBSR No. B1320133020.

Fuzzy logic systems (FLSs) have been widely utilized for dealing with uncertainties. Compared with type-1 fuzzy logic systems (T1-FLSs), which use only type-1 fuzzy sets (T1-FSs), type-2 fuzzy logic systems (T2-FLSs), which use at least one type-2 fuzzy set (T2-FS), have stronger capability of modeling vagueness and unreliability of information [6]. Considering the computational costs in real time control, interval type-2 fuzzy logic systems (IT2-FLSs), which use interval type-2 fuzzy sets (IT2-FSs) instead, have attracted more attention than general T2-FLSs.

In this paper, an adaptive interval type-2 fuzzy output feedback control (AIT2-FOFC) scheme is proposed for FAHVs in the presence of unknown flexibilities and parameter uncertainties. After calculating the derivatives of the velocity and altitude repeatedly, the FAHV longitudinal model is completely input-output linearized. Due to the unmeasurable high order derivatives of the outputs, the design can be separated into two tasks based on the separate principle. First, a state feedback dynamic inversion controller is formulated as the basic nominal controller to stabilize the system. An adaptive interval type-2 fuzzy logic system (AIT2-FLS) is further constructed to approximate the unknown uncertainties in the FAHV longitudinal model. Then, a nonlinear high gain observer is applied to directly estimate the unavailable high order derivatives of the velocity tracking error and altitude tracking error. The whole AIT2-FOFC scheme is finally achieved through combining the state feedback controller and the nonlinear high gain observer. Simulation results validate the robustness of our AIT2-FOFC scheme against unknown flexible dynamics as well as parameter uncertainties.

The rest of this paper is organized as follows. Section 2 briefly states the preliminaries of this study. From Section 3

to Section 5, we introduce our design process in details, including output feedback formulation, state feedback control design and AIT2-FOFC design. Simulation results are presented in Section 6, after which we draw our conclusions.

2 PRELIMINARIES

2.1 Longitudinal Dynamics of FAHV

In this paper, the following nonlinear longitudinal dynamics of the FAHV, which contain five rigid-body states and six flexible states, are considered [7]:

$$\dot{V} = \left(T\cos\alpha - D\right)/m - g\sin\gamma \tag{1}$$

$$\dot{\gamma} = \left(L + T\sin\alpha\right)/mV - g\cos\gamma/V \tag{2}$$

$$\dot{h} = V\sin\gamma \tag{3}$$

$$\dot{\alpha} = q - \dot{\gamma} \tag{4}$$

$$\dot{q} = M_{yy} / I_{yy} \tag{5}$$

$$\ddot{\eta}_i = -2\zeta_i\omega_i\dot{\eta}_i - \omega_i^2\eta_i + N_i, \quad i = 1,2,3 \tag{6}$$

where V denotes the velocity, γ denotes the flight path angle, h denotes the altitude, α denotes the angle of attack, q denotes the pitch rate, and $\boldsymbol{\eta} = [\eta_1\ \dot{\eta}_1\ \eta_2\ \dot{\eta}_2\ \eta_3\ \dot{\eta}_3]^T$ stands for the first three flexible modes. L, D, T and M_{yy} represent the lift, the drag, the thrust and the pitching moment, respectively, while N_1, N_2 and N_3 are the three generalized forces. The approximate expressions of the above terms are given as follows:

$$L \approx 0.5\rho V^2 s C_L(\alpha, \boldsymbol{\delta}, \boldsymbol{\eta}) \tag{7}$$

$$D \approx 0.5\rho V^2 s C_D(\alpha, \boldsymbol{\delta}, \boldsymbol{\eta}) \tag{8}$$

$$T \approx 0.5\rho V^2 s\left[C_{T,\phi}(\alpha)\phi + C_T(\alpha) + \boldsymbol{C}_T^{\eta}\boldsymbol{\eta}\right] \tag{9}$$

$$M_{yy} \approx z_T T + 0.5\rho V^2 s\bar{c} C_M(\alpha, \boldsymbol{\delta}, \boldsymbol{\eta}) \tag{10}$$

$$\begin{aligned} N_i \approx 0.5\rho V^2 s\Big[& N_i^{\alpha^2}\alpha^2 + N_i^{\alpha}\alpha + N_i^{\delta_e}\delta_e + N_i^{\delta_c}\delta_c \\ & + N_i^0 + \boldsymbol{N}_i^{\eta}\boldsymbol{\eta}\Big] \end{aligned} \tag{11}$$

where $\boldsymbol{\delta} = [\delta_c, \delta_e]^T$ represents the canard deflection and elevator deflection respectively, ϕ denotes the throttle setting, and

$$C_{T,\phi}(\alpha) = C_T^{\phi\alpha^3}\alpha^3 + C_T^{\phi\alpha^2}\alpha^2 + C_T^{\phi\alpha}\alpha + C_T^{\phi} \tag{12}$$

$$C_T(\alpha) = C_T^3\alpha^3 + C_T^2\alpha^2 + C_T^1\alpha + C_T^0 \tag{13}$$

$$C_L(\alpha, \boldsymbol{\delta}, \boldsymbol{\eta}) = C_L^{\alpha}\alpha + C_L^{\delta_e}\delta_e + C_L^{\delta_c}\delta_c + C_L^0 + \boldsymbol{C}_L^{\eta}\boldsymbol{\eta} \tag{14}$$

$$\begin{aligned} C_D(\alpha, \boldsymbol{\delta}, \boldsymbol{\eta}) = {} & C_D^{\alpha^2}\alpha^2 + C_D^{\alpha}\alpha + C_D^{\delta_e^2}\delta_e^2 + C_D^{\delta_e}\delta_e + C_D^{\delta_c^2}\delta_c^2 \\ & + C_D^{\delta_c}\delta_c + C_D^0 + \boldsymbol{C}_D^{\eta}\boldsymbol{\eta} \end{aligned} \tag{15}$$

$$\begin{aligned} C_M(\alpha, \boldsymbol{\delta}, \boldsymbol{\eta}) = {} & C_M^{\alpha^2}\alpha^2 + C_M^{\alpha}\alpha + C_M^{\delta_e}\delta_e + C_M^{\delta_c}\delta_c + C_M^0 \\ & + \boldsymbol{C}_M^{\eta}\boldsymbol{\eta} \end{aligned} \tag{16}$$

$$\boldsymbol{C}_j^{\eta} = \left[C_j^{\eta_1}\quad 0\quad C_j^{\eta_2}\quad 0\quad C_j^{\eta_3}\quad 0\right], \quad j = T, L, D, M \tag{17}$$

$$\boldsymbol{N}_i^{\eta} = \left[N_i^{\eta_1}\quad 0\quad N_i^{\eta_2}\quad 0\quad N_i^{\eta_3}\quad 0\right], \quad i = 1,2,3. \tag{18}$$

Moreover, the canard deflection δ_c is set to be ganged with the elevator deflection δ_e, with the relationship of $\delta_c = k_{ec}\delta_e = -\left(C_L^{\delta_e}/C_L^{\delta_c}\right)\delta_e$ [8].

The engine dynamics can be described by a second-order system using a new control input ϕ_c:

$$\ddot{\phi} = -2\zeta_n\omega_n\dot{\phi} - \omega_n^2\phi + \omega_n^2\phi_c. \tag{19}$$

For detail information about each parameter, the reader can refer to [9].

2.2 Brief Description of IT2-FLS

In this study, IT2-FLS is employed to approximate the flexibilities as well as the unknown uncertainties in the FAHV longitudinal model. The structure of IT2-FLS is displayed in Fig 1. It mainly consists of four parts: fuzzifier, rule bases, inference and output processing. Different from T1-FLS, at least one IT2-FS is employed in the rule bases of IT2-FLS, which enhances the ability of handling complex uncertainties. Besides, in the output processing part, the type reducer first maps the IT2 fuzzy output sets into T1-FSs, and then the crisp outputs can be obtained after defuzzification.

For a Mamdani IT2-FLS with p inputs $x_{f1} \in X_1, \ldots,$ $x_{fp} \in X_p$ and one output $u \in U$, the sth rule can be expressed as follows:

$$\begin{aligned} R^s: {} & IF\ x_{f1}\ is\ \tilde{F}_1^s\ and\ \ldots and\ x_{fp}\ is\ \tilde{F}_p^s, \\ & THEN\ u\ is\ \tilde{G}^s \qquad s = 1, 2, \ldots, M \end{aligned} \tag{20}$$

where $\tilde{F}_m^s$ $(m = 1, 2, \ldots, p)$ is the antecedent IT2-FS, with the upper membership function (UMF) and lower membership function (LMF) of $\bar{\mu}_{\tilde{F}_m^s}(x_{fm})$ and $\underline{\mu}_{\tilde{F}_m^s}(x_{fm})$ respectively, while $\tilde{G}^s$ is the consequent IT2-FS, with the corresponding centroid of θ^s. Then, if we use singleton fuzzification and product inference, the degree of firing $f^s(x_{f1}, \ldots, x_{fp})$ can be written as follows:

$$\begin{aligned} f^s(x_{f1}, \ldots, x_{fp}) &\in \left[\underline{f}^s(x_{f1}, \ldots, x_{fp}), \bar{f}^s(x_{f1}, \ldots, x_{fp})\right] \\ &= \left[\prod_{m=1}^{p}\underline{\mu}_{\tilde{F}_m^s}(x_{fm}), \prod_{m=1}^{p}\bar{\mu}_{\tilde{F}_m^s}(x_{fm})\right]. \end{aligned} \tag{21}$$

Define the fuzzy basic function (FBF) as follows:

$$\xi^s = f^s(x_{f1}, \ldots, x_{fp}) \Big/ \sum_{s=1}^{M} f^s(x_{f1}, \ldots, x_{fp}). \tag{22}$$

Finally, by applying center-of-sets type reduction and center average defuzzification, we can obtain the crisp output of IT2-FLS:

$$u = \left(\boldsymbol{\theta}^T\boldsymbol{\xi}_l + \boldsymbol{\theta}^T\boldsymbol{\xi}_r\right)/2 = \boldsymbol{\theta}^T\left(\boldsymbol{\xi}_l + \boldsymbol{\xi}_r\right)/2 = \boldsymbol{\theta}^T\boldsymbol{\xi} \tag{23}$$

where $\boldsymbol{\theta} = \left[\theta^1, \ldots, \theta^M\right]^T$ and $\boldsymbol{\xi} = \left(\boldsymbol{\xi}_l + \boldsymbol{\xi}_r\right)/2$. Besides, $\boldsymbol{\xi}_l = \left[\xi_l^1, \ldots, \xi_l^M\right]^T$ and $\boldsymbol{\xi}_r = \left[\xi_r^1, \ldots, \xi_r^M\right]^T$ are the boundary FBF vectors which can be calculated through the Karnik-Mendel algorithm [10].

For the IT2-FLS's capability of approximating a real continuous function on a compact domain, we have the following IT2-FLS approximation theorem:

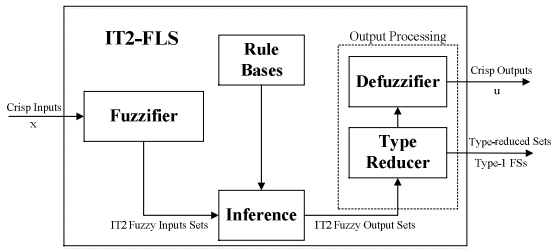

Fig 1. The structure of IT2-FLS.

Theorem 1 [11]: The IT2-FLS can uniformly approximate any function $f(\boldsymbol{x})$ which is continuous in $C^r[-1,1]$ to any degree of accuracy. In other words, for $\forall \varepsilon > 0$, there exists an IT2-FLS as (23) such that

$$\sup_{x \in C^r[-1,1]} \left| f(\boldsymbol{x}) - \boldsymbol{\theta}^T \boldsymbol{\xi}(\boldsymbol{x}) \right| < \varepsilon. \tag{24}$$

3 OUTPUT FEEDBACK FORMULATION

The control objective of this paper is to design an output feedback control scheme which can make the velocity *V* and altitude *h* of the FAHV track the reference commands V_c and h_c respectively in the presence of unknown flexibilities as well as parameter uncertainties. In the following three sections, we will introduce our proposed control scheme in details, including output feedback formulation, state feedback control design and AIT2-FOFC design.

The overall control scheme is depicted in Fig 2. For the FAHV longitudinal model, the control inputs are $\boldsymbol{u} = [\phi_c, \delta_e]^T$, while the system outputs are $\boldsymbol{y} = [V, h]^T$. Besides, since the measurements of flexible dynamics are difficult and costly, here we treat them unknown.

It is not difficult to find that the nonlinear longitudinal dynamics of the FAHV (1)-(6) satisfy the relative degree condition [12]. Therefore, the system can be completely input-output linearized. After differentiating *V* and *h* three times and four times respectively, the FAHV longitudinal dynamics can be transformed into the following affine nonlinear form:

$$\begin{bmatrix} \dddot{V} \\ h^{(4)} \end{bmatrix} = \begin{bmatrix} f_v \\ f_h \end{bmatrix} + \begin{bmatrix} b_{11} & b_{12} \\ b_{21} & b_{22} \end{bmatrix} \begin{bmatrix} \phi_c \\ \delta_e \end{bmatrix} \tag{25}$$

where

$$f_v = \left(\omega_1 \ddot{\boldsymbol{x}}_0 + \dot{\boldsymbol{x}}^T \Omega_2 \dot{\boldsymbol{x}} \right) / m \tag{26}$$

$$\begin{aligned} f_h = {} & \left(\omega_1 \ddot{\boldsymbol{x}}_0 + \dot{\boldsymbol{x}}^T \Omega_2 \dot{\boldsymbol{x}} \right) \sin\gamma / m + V \left(\pi_1 \ddot{\boldsymbol{x}}_0 + \dot{\boldsymbol{x}}^T \Pi_2 \dot{\boldsymbol{x}} \right) \cos\gamma \\ & + 3\ddot{V}\dot{\gamma}\cos\gamma - 3\dot{V}\dot{\gamma}^2 \sin\gamma + 3\dot{V}\ddot{\gamma}\cos\gamma \\ & - 3V\dot{\gamma}\ddot{\gamma}\sin\gamma - V\dot{\gamma}^3 \cos\gamma \end{aligned} \tag{27}$$

$$b_{11} = \frac{\omega_n^2}{m} \frac{\partial T}{\partial \phi} \cos\alpha \tag{28}$$

$$b_{12} = \frac{\rho V^2 s\bar{c}}{2mI_{yy}} \left(\frac{\partial T}{\partial \alpha} \cos\alpha - T\sin\alpha - \frac{\partial D}{\partial \alpha} \right) \left(C_M^{\delta_e} - \frac{C_L^{\delta_e}}{C_L^{\delta_c}} C_M^{\delta_c} \right) \tag{29}$$

$$b_{21} = \frac{\omega_n^2}{m} \frac{\partial T}{\partial \phi} \sin(\gamma + \alpha) \tag{30}$$

$$\begin{aligned} b_{22} = {} & \frac{\rho V^2 s\bar{c}}{2mI_{yy}} \left[\left(\frac{\partial T}{\partial \alpha} \cos\alpha - T\sin\alpha - \frac{\partial D}{\partial \alpha} \right) \sin\gamma \right. \\ & \left. + \left(\frac{\partial L}{\partial \alpha} + \frac{\partial T}{\partial \alpha} \sin\alpha + T\cos\alpha \right) \cos\gamma \right] \left(C_M^{\delta_e} - \frac{C_L^{\delta_e}}{C_L^{\delta_c}} C_M^{\delta_c} \right) \end{aligned} \tag{31}$$

in which $\boldsymbol{x} = [V \ \gamma \ \alpha \ \phi \ h]^T$ and $\ddot{\boldsymbol{x}}_0 = \left[\ddot{V} \ \ddot{\gamma} \ \ddot{\alpha}_0 \ \ddot{\phi}_0 \ \ddot{h} \right]^T$.

Although input-output linearization makes the control problem less complicated, the accurate model information is needed during the control development. In addition, high order derivatives of the velocity and altitude are necessary as well, which are not measurable from the on-board sensors. When complex nonlinear uncertainties exist, these values even become incomputable. Motivated by the results in [5, 13], we can separate the design into two tasks based on the separation principle. First, a state feedback controller is developed to stabilize the system, which will be introduced in Section 4. Then, a nonlinear high gain observer is applied to estimate the high order derivatives of the velocity tracking error and altitude tracking error, which can be seen in Section 5.

4 STATE FEEDBACK CONTROL DESIGN

4.1 Dynamic Inversion Controller Design

Considering the effects of unknown flexible dynamics and parameter uncertainties, we rewrite (25) in the following form:

$$\begin{bmatrix} \dddot{V} \\ h^{(4)} \end{bmatrix} = \begin{bmatrix} f_v \\ f_h \end{bmatrix} + \begin{bmatrix} b_{11} & b_{12} \\ b_{21} & b_{22} \end{bmatrix} \begin{bmatrix} \phi_c \\ \delta_e \end{bmatrix} + \begin{bmatrix} \Delta_v \\ \Delta_h \end{bmatrix} = \boldsymbol{F} + \boldsymbol{B}\boldsymbol{u} \tag{32}$$

where

$$\boldsymbol{F} = \begin{bmatrix} F_v \\ F_h \end{bmatrix} = \begin{bmatrix} f_v + \Delta_v \\ f_h + \Delta_h \end{bmatrix}, \quad \boldsymbol{B} = \begin{bmatrix} b_{11} & b_{12} \\ b_{21} & b_{22} \end{bmatrix}, \tag{33}$$

Δ_v and Δ_h denote the total unknown uncertainties, including flexibilities and parameter uncertainties, in the velocity channel and altitude channel, respectively. Let

$$\boldsymbol{e}_v = \left(e_{v0}, e_{v1}, e_{v2} \right)^T = \left(e_v, \dot{e}_v, \ddot{e}_v \right)^T \tag{34}$$

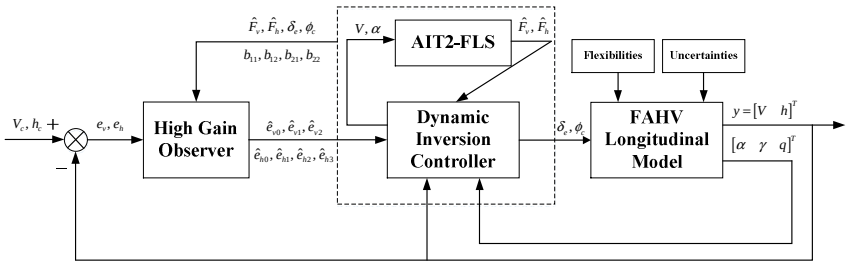

Fig 2. The block diagram of the AIT2-FOFC scheme.

$$\boldsymbol{e}_h = \left(e_{h0}, e_{h1}, e_{h2}, e_{h3}\right)^T = \left(e_h, \dot{e}_h, \ddot{e}_h, \dddot{e}_h\right)^T \quad (35)$$

where $e_v = V - V_c$ and $e_h = h - h_c$ are the velocity tracking error and altitude tracking error respectively. Suppose $\boldsymbol{B}$ is invertible, then the dynamic inversion controller, which can lead to the exponentially stable dynamics, can be formulated as the basic controller:

$$\boldsymbol{u} = \begin{bmatrix} \phi_c \\ \delta_e \end{bmatrix} = \begin{bmatrix} b_{11} & b_{12} \\ b_{21} & b_{22} \end{bmatrix}^{-1} \begin{bmatrix} -F_v - \sum_{i=0}^{2} k_{1i} e_{vi} + \dddot{V}_c \\ -F_h - \sum_{j=0}^{3} k_{2j} e_{hj} + h_c^{(4)} \end{bmatrix} \quad (36)$$

where k_{1i} $(i = 0, 1, 2)$ and k_{2j} $(j = 0, 1, 2, 3)$ are set as the coefficients of Hurwitz polynomials.

4.2 AIT2-FLS Design

Since $\boldsymbol{F} = \left[F_v, F_h\right]^T$ contains unknown model uncertainties Δ_v and Δ_h, the accurate values of $\boldsymbol{F}$ is unavailable in reality. Thus, here we use AIT2-FLS to estimate the uncertain term $\boldsymbol{F}$, and (36) becomes:

$$\boldsymbol{u} = \begin{bmatrix} \phi_c \\ \delta_e \end{bmatrix} = \begin{bmatrix} b_{11} & b_{12} \\ b_{21} & b_{22} \end{bmatrix}^{-1} \begin{bmatrix} -\hat{F}_v - \sum_{i=0}^{2} k_{1i} e_{vi} + \dddot{V}_c \\ -\hat{F}_h - \sum_{j=0}^{3} k_{2j} e_{hj} + h_c^{(4)} \end{bmatrix} \quad (37)$$

where $\hat{F}_v$ and $\hat{F}_h$ denote the outputs of IT2-FLS. According to the detail expressions of the FAHV longitudinal model (1)-(18), a two-inputs two-outputs IT2-FLS can be constructed, with the rule bases of:

$$\begin{aligned} R^s &: \textit{IF } x_{f1} \textit{ is } \tilde{F}_1^s \textit{ and } x_{f2} \textit{ is } \tilde{F}_2^s, \\ &\textit{THEN } \hat{F}_v \textit{ is } G_1^s \textit{ and } \hat{F}_h \textit{ is } G_2^s, \quad s = 1, 2, ..., M \end{aligned} \quad (38)$$

where V and α are chosen for x_{f1} and x_{f2} respectively. The antecedent fuzzy sets $\tilde{F}_1^s$ and $\tilde{F}_2^s$ are set as Gaussian IT2-FSs, whose LMFs and UMFs are:

$$\underline{\mu}_{\tilde{F}_m^s}(x_{fm}) = \exp\left(-\left(x_{fm} - \underline{m}_{\tilde{F}_m^s}\right)^2 \Big/ 2\underline{\sigma}_{\tilde{F}_m^s}^2\right) \quad (39)$$

$$\overline{\mu}_{\tilde{F}_m^s}(x_{fm}) = \exp\left(-\left(x_{fm} - \overline{m}_{\tilde{F}_m^s}\right)^2 \Big/ 2\overline{\sigma}_{\tilde{F}_m^s}^2\right), \quad m = 1, 2 \quad (40)$$

respectively, while the consequent fuzzy sets G_1^s and G_2^s are Gaussian T1-FSs, with the corresponding centroids of θ_v^s and θ_h^s respectively. Then, if we use singleton fuzzification, product inference, center-of-sets type reduction and center average defuzzification, the estimation of F_v and F_h can be obtained:

$$\hat{F}_v = \boldsymbol{\theta}_v^T \boldsymbol{\xi}_v, \quad \hat{F}_h = \boldsymbol{\theta}_h^T \boldsymbol{\xi}_h. \quad (41)$$

Let

$$\boldsymbol{A}_v = \begin{bmatrix} 0 & 1 & 0 \\ 0 & 0 & 1 \\ -k_{10} & -k_{11} & -k_{12} \end{bmatrix}, \ \boldsymbol{b}_v = \begin{bmatrix} 0 \\ 0 \\ 1 \end{bmatrix}, \quad (42)$$

$$\boldsymbol{A}_h = \begin{bmatrix} 0 & 1 & 0 & 0 \\ 0 & 0 & 1 & 0 \\ 0 & 0 & 0 & 1 \\ -k_{20} & -k_{21} & -k_{22} & -k_{23} \end{bmatrix}, \ \boldsymbol{b}_h = \begin{bmatrix} 0 \\ 0 \\ 0 \\ 1 \end{bmatrix}. \quad (43)$$

Then substituting (41) into (37), we can obtain the following state feedback control algorithm:

$$\boldsymbol{u} = \begin{bmatrix} \phi_c \\ \delta_e \end{bmatrix} = \begin{bmatrix} b_{11} & b_{12} \\ b_{21} & b_{22} \end{bmatrix}^{-1} \begin{bmatrix} -\boldsymbol{\theta}_v^T \boldsymbol{\xi}_v - \sum_{i=0}^{2} k_{1i} e_{vi} + \dddot{V}_c \\ -\boldsymbol{\theta}_h^T \boldsymbol{\xi}_h - \sum_{j=0}^{3} k_{2j} e_{hj} + h_c^{(4)} \end{bmatrix}. \quad (44)$$

The adaptive laws for $\boldsymbol{\theta}_v$ and $\boldsymbol{\theta}_h$ can be designed as:

$$\dot{\boldsymbol{\theta}}_v = \gamma_v \boldsymbol{e}_v^T \boldsymbol{P}_v \boldsymbol{b}_v \boldsymbol{\xi}_v - \sigma_v \left(\boldsymbol{\theta}_v - \boldsymbol{\theta}_v^0\right) \quad (45)$$

$$\dot{\boldsymbol{\theta}}_h = \gamma_h \boldsymbol{e}_h^T \boldsymbol{P}_h \boldsymbol{b}_h \boldsymbol{\xi}_h - \sigma_h \left(\boldsymbol{\theta}_h - \boldsymbol{\theta}_h^0\right) \quad (46)$$

where $\gamma_v > 0$, $\gamma_h > 0$, $\sigma_v > 0$ and $\sigma_h > 0$. $\boldsymbol{\theta}_v^0$ and $\boldsymbol{\theta}_h^0$ are the predefined consequent centroid vectors. Besides, $\boldsymbol{P}_v$ and $\boldsymbol{P}_h$ are the positive definite matrix solutions of the following Lyapunov functions:

$$\boldsymbol{A}_v^T \boldsymbol{P}_v + \boldsymbol{P}_v \boldsymbol{A}_v = -\boldsymbol{Q}_v, \quad \boldsymbol{A}_h^T \boldsymbol{P}_h + \boldsymbol{P}_h \boldsymbol{A}_h = -\boldsymbol{Q}_h \quad (47)$$

where $\boldsymbol{Q}_v$ and $\boldsymbol{Q}_h$ are appropriate positive definite square matrices.

Remark 1: The σ-modification terms of the form $-\sigma_v \left(\boldsymbol{\theta}_v - \boldsymbol{\theta}_v^0\right)$ and $-\sigma_h \left(\boldsymbol{\theta}_h - \boldsymbol{\theta}_h^0\right)$ in the adaptive laws (45) and (46) can keep the adaptive parameters $\boldsymbol{\theta}_v$ and $\boldsymbol{\theta}_h$ in bound in the presence of model uncertainties. Besides, the better approximation of the optimal estimation vectors we make $\boldsymbol{\theta}_v^0$ and $\boldsymbol{\theta}_h^0$, the less tracking errors will be.

4.3 Stability Analysis

This subsection will explore the stability of the above state feedback control scheme. First, we define $\boldsymbol{\theta}_v^*$ and $\boldsymbol{\theta}_h^*$ as the optimal estimation vectors, while ε_v and ε_h as the minimal estimation errors. Then, F_v and F_h in (33) can be written in the following form:

$$F_v = \boldsymbol{\theta}_v^{*T} \boldsymbol{\xi}_v + \varepsilon_v, \quad F_h = \boldsymbol{\theta}_h^{*T} \boldsymbol{\xi}_h + \varepsilon_h. \quad (48)$$

Next, combining (32), (44) and (48), the overall error dynamics of the system can be obtained:

$$\dot{\boldsymbol{e}}_v = \boldsymbol{A}_v \boldsymbol{e}_v + \boldsymbol{b}_v \left(\tilde{\boldsymbol{\theta}}_v^T \boldsymbol{\xi}_v + \varepsilon_v\right) \quad (49)$$

$$\dot{\boldsymbol{e}}_h = \boldsymbol{A}_h \boldsymbol{e}_h + \boldsymbol{b}_h \left(\tilde{\boldsymbol{\theta}}_h^T \boldsymbol{\xi}_h + \varepsilon_h\right) \quad (50)$$

where $\tilde{\boldsymbol{\theta}}_v = \boldsymbol{\theta}_v - \boldsymbol{\theta}_v^*$ and $\tilde{\boldsymbol{\theta}}_h = \boldsymbol{\theta}_h - \boldsymbol{\theta}_h^*$. Finally, the stability characteristic is explored through the following theorem.

Theorem 2: Consider the state feedback closed-loop system consisting of the FAHV longitudinal model (1)-(6), the control algorithm (44), together with the adaptive laws (45) and (46). Then, both the velocity tracking error and altitude tracking error are uniformly ultimately bounded (UUB).

Proof: Choose the following Lyapunov function:

$$V = \frac{1}{2} \boldsymbol{e}_v^T \boldsymbol{P}_v \boldsymbol{e}_v + \frac{1}{2} \boldsymbol{e}_h^T \boldsymbol{P}_h \boldsymbol{e}_h + \frac{1}{2\gamma_v} \tilde{\boldsymbol{\theta}}_v^T \tilde{\boldsymbol{\theta}}_v + \frac{1}{2\gamma_h} \tilde{\boldsymbol{\theta}}_h^T \tilde{\boldsymbol{\theta}}_h. \quad (51)$$

Taking the time derivative of V, we can obtain

$$\begin{aligned} \dot{V} = &-\frac{1}{2} \boldsymbol{e}_v^T \boldsymbol{Q}_v \boldsymbol{e}_v + \boldsymbol{e}_v^T \boldsymbol{P}_v \boldsymbol{b}_v \varepsilon_v + \boldsymbol{e}_v^T \boldsymbol{P}_v \boldsymbol{b}_v \tilde{\boldsymbol{\theta}}_v^T \boldsymbol{\xi}_v - \boldsymbol{e}_v^T \boldsymbol{P}_v \boldsymbol{b}_v \tilde{\boldsymbol{\theta}}_v^T \boldsymbol{\xi}_v \\ &- \frac{\sigma_v}{\gamma_v} \tilde{\boldsymbol{\theta}}_v^T \left(\boldsymbol{\theta}_v - \boldsymbol{\theta}_v^0\right) - \frac{1}{2} \boldsymbol{e}_h^T \boldsymbol{Q}_h \boldsymbol{e}_h + \boldsymbol{e}_h^T \boldsymbol{P}_h \boldsymbol{b}_h \varepsilon_h \\ &+ \boldsymbol{e}_h^T \boldsymbol{P}_h \boldsymbol{b}_h \tilde{\boldsymbol{\theta}}_h^T \boldsymbol{\xi}_h - \boldsymbol{e}_h^T \boldsymbol{P}_h \boldsymbol{b}_h \tilde{\boldsymbol{\theta}}_h^T \boldsymbol{\xi}_h - \frac{\sigma_v}{\gamma_v} \tilde{\boldsymbol{\theta}}_h^T \left(\boldsymbol{\theta}_h - \boldsymbol{\theta}_h^0\right) \end{aligned} \quad (52)$$

$$= -\frac{1}{2}\boldsymbol{e}_v^T\boldsymbol{Q}_v\boldsymbol{e}_v + \boldsymbol{e}_v^T\boldsymbol{P}_v\boldsymbol{b}_v\varepsilon_v - \frac{1}{2}\boldsymbol{e}_h^T\boldsymbol{Q}_h\boldsymbol{e}_h + \boldsymbol{e}_h^T\boldsymbol{P}_h\boldsymbol{b}_h\varepsilon_h$$
$$-\frac{\sigma_v}{\gamma_v}\tilde{\boldsymbol{\theta}}_v^T\left[\tilde{\boldsymbol{\theta}}_v - \left(\boldsymbol{\theta}_v^0 - \boldsymbol{\theta}_v^*\right)\right] - \frac{\sigma_v}{\gamma_v}\tilde{\boldsymbol{\theta}}_h^T\left[\tilde{\boldsymbol{\theta}}_h - \left(\boldsymbol{\theta}_h^0 - \boldsymbol{\theta}_h^*\right)\right].$$

Since

$$\tilde{\boldsymbol{\theta}}_v^T\left[\tilde{\boldsymbol{\theta}}_v - \left(\boldsymbol{\theta}_v^0 - \boldsymbol{\theta}_v^*\right)\right] \le -\frac{1}{2}\tilde{\boldsymbol{\theta}}_v^T\tilde{\boldsymbol{\theta}}_v + \frac{1}{2}\left\|\boldsymbol{\theta}_v^0 - \boldsymbol{\theta}_v^*\right\|^2, \quad (53)$$

$$\tilde{\boldsymbol{\theta}}_h^T\left[\tilde{\boldsymbol{\theta}}_h - \left(\boldsymbol{\theta}_h^0 - \boldsymbol{\theta}_h^*\right)\right] \le -\frac{1}{2}\tilde{\boldsymbol{\theta}}_h^T\tilde{\boldsymbol{\theta}}_h + \frac{1}{2}\left\|\boldsymbol{\theta}_h^0 - \boldsymbol{\theta}_h^*\right\|^2, \quad (54)$$

the last equality of (52) is derived as

$$\begin{aligned}\dot{V} \le & -\frac{1}{2}\boldsymbol{e}_v^T\boldsymbol{Q}_v\boldsymbol{e}_v + \boldsymbol{e}_v^T\boldsymbol{P}_v\boldsymbol{b}_v\varepsilon_v - \frac{1}{2}\boldsymbol{e}_h^T\boldsymbol{Q}_h\boldsymbol{e}_h + \boldsymbol{e}_h^T\boldsymbol{P}_h\boldsymbol{b}_h\varepsilon_h \\ & -\frac{\sigma_v}{2\gamma_v}\tilde{\boldsymbol{\theta}}_v^T\tilde{\boldsymbol{\theta}}_v + \frac{\sigma_v}{2\gamma_v}\left\|\boldsymbol{\theta}_v^0 - \boldsymbol{\theta}_v^*\right\|^2 - \frac{\sigma_h}{2\gamma_h}\tilde{\boldsymbol{\theta}}_h^T\tilde{\boldsymbol{\theta}}_h \\ & +\frac{\sigma_h}{2\gamma_h}\left\|\boldsymbol{\theta}_h^0 - \boldsymbol{\theta}_h^*\right\|^2 \\ = & -\frac{1}{2}\boldsymbol{e}_v^T\boldsymbol{Q}_v\boldsymbol{e}_v - \frac{1}{2}\boldsymbol{e}_h^T\boldsymbol{Q}_h\boldsymbol{e}_h - \frac{\sigma_v}{2\gamma_v}\tilde{\boldsymbol{\theta}}_v^T\tilde{\boldsymbol{\theta}}_v - \frac{\sigma_h}{2\gamma_h}\tilde{\boldsymbol{\theta}}_h^T\tilde{\boldsymbol{\theta}}_h + W\end{aligned} \quad (55)$$

where

$$\begin{aligned}W = & \boldsymbol{e}_v^T\boldsymbol{P}_v\boldsymbol{b}_v\varepsilon_v + \boldsymbol{e}_h^T\boldsymbol{P}_h\boldsymbol{b}_h\varepsilon_h + \frac{\sigma_v}{2\gamma_v}\left\|\boldsymbol{\theta}_v^0 - \boldsymbol{\theta}_v^*\right\|^2 \\ & +\frac{\sigma_h}{2\gamma_h}\left\|\boldsymbol{\theta}_h^0 - \boldsymbol{\theta}_h^*\right\|^2\end{aligned} \quad (56)$$

is a bounded term. By choosing $\mu_1 = \underline{\lambda}(\boldsymbol{Q}_v)/\overline{\lambda}(\boldsymbol{P}_v)$, $\mu_2 = \underline{\lambda}(\boldsymbol{Q}_h)/\overline{\lambda}(\boldsymbol{P}_h)$, $\mu_3 = \sigma_v$ and $\mu_4 = \sigma_h$, where $\underline{\lambda}$ and $\overline{\lambda}$ denote the minimum and maximum eigenvalues respectively, we have

$$\dot{V} \le -\mu V + W \quad (57)$$

with $\mu = \min\left(\mu_1, \mu_2, \mu_3, \mu_4\right)$. Therefore, both the velocity tracking error and altitude tracking error are UUB. This completes the proof.

5 AIT2-FOFC DESIGN

As mentioned in Section 3, it is very hard to obtain the high order derivatives of the velocity and altitude in real applications. Thus, we employ the following nonlinear high gain observer to directly estimate the unmeasurable states $\boldsymbol{e}_v$ and $\boldsymbol{e}_h$ which are used in (44):

$$\dot{\hat{e}}_{v0} = \hat{e}_{v1} + \alpha_{v1}\left(e_{v0} - \hat{e}_{v0}\right)/\varepsilon_v \quad (58)$$

$$\dot{\hat{e}}_{v1} = \hat{e}_{v2} + \alpha_{v2}\left(e_{v0} - \hat{e}_{v0}\right)/\varepsilon_v^2 \quad (59)$$

$$\dot{\hat{e}}_{v2} = \boldsymbol{\theta}_v^T\boldsymbol{\xi}_v + b_{11}\phi_c + b_{12}\delta_e + \alpha_{v3}\left(e_{v0} - \hat{e}_{v0}\right)/\varepsilon_v^3 \quad (60)$$

where $\hat{e}_{vi}$ $(i = 0, 1, 2)$ is the estimation of e_{vi}, ε_v is a small positive constant, $\alpha_{v(i+1)}$ is set as the coefficient of Hurwitz polynomial. In the same way,

$$\dot{\hat{e}}_{h0} = \hat{e}_{h1} + \alpha_{h1}\left(e_{h0} - \hat{e}_{h0}\right)/\varepsilon_h \quad (61)$$

$$\dot{\hat{e}}_{h1} = \hat{e}_{h2} + \alpha_{h2}\left(e_{h0} - \hat{e}_{h0}\right)/\varepsilon_h^2 \quad (62)$$

$$\dot{\hat{e}}_{h2} = \hat{e}_{h3} + \alpha_{h3}\left(e_{h0} - \hat{e}_{h0}\right)/\varepsilon_h^3 \quad (63)$$

$$\dot{\hat{e}}_{h3} = \boldsymbol{\theta}_h^T\boldsymbol{\xi}_h + b_{21}\phi_c + b_{22}\delta_e + \alpha_{h4}\left(e_{h0} - \hat{e}_{h0}\right)/\varepsilon_h^4 \quad (64)$$

where $\hat{e}_{hj}$ $(j = 0, 1, 2, 3)$ is the estimation of e_{hj}, ε_h is a small positive constant, $\alpha_{h(j+1)}$ is set as the coefficient of Hurwitz polynomial. The stability analysis of the above nonlinear high gain observer can refer to [13]. After replacing e_{vi} and e_{hj} in (44) by $\hat{e}_{vi}$ and $\hat{e}_{hj}$ respectively, we finally obtain our AIT2-FOFC scheme based on the separation principle:

$$\boldsymbol{u} = \begin{bmatrix}\phi_c \\ \delta_e\end{bmatrix} = \begin{bmatrix}b_{11} & b_{12} \\ b_{21} & b_{22}\end{bmatrix}^{-1}\begin{bmatrix}-\boldsymbol{\theta}_v^T\boldsymbol{\xi}_v - \sum_{i=0}^{2}k_{1i}\hat{e}_{vi} + \dddot{V}_c \\ -\boldsymbol{\theta}_h^T\boldsymbol{\xi}_h - \sum_{j=0}^{3}k_{2j}\hat{e}_{hj} + h_c^{(4)}\end{bmatrix}. \quad (65)$$

6 SIMULATION

To validate the effectiveness of our AIT2-FOFC scheme, the results of the numerical simulation are presented in this section. The trimmed cruise conditions of the simulation are selected as $V_0 = 7846.4\,ft/s$, $\gamma_0 = 0rad$, $h_0 = 85000\,ft$, $\alpha_0 = 0.0219rad$, $q_0 = 0rad/s$, η_1=0.594$ft\sqrt{slug}$, η_2 = –0.0976 $ft\sqrt{slug}$, η_3 = – 0.0335 $ft\sqrt{slug}$ and $\dot{\eta}_1 = \dot{\eta}_2 = \dot{\eta}_3 = 0$ $ft\sqrt{slug}/s$. 300*ft/s* step signal and 1800*ft* step signal are chosen as the velocity reference command and altitude reference command respectively. In order to arrange a better transition process, we employ the tracking differentiators as follows [14]:

$$\begin{cases} fs_1(N) = -\lambda_v\left(\lambda_v\left(\lambda_v\left(V_c(N) - V_r\right) + 3\dot{V}_c(N)\right) + 3\ddot{V}_c(N)\right) \\ V_c(N+1) = V_c(N) + \tau * \dot{V}_c(N) \\ \dot{V}_c(N+1) = \dot{V}_c(N) + \tau * \ddot{V}_c(N) \\ \ddot{V}_c(N+1) = \ddot{V}_c(N) + \tau * fs_1(N) \end{cases} \quad (66)$$

$$\begin{cases} fs_2(N) = -\lambda_h\left(\lambda_h\left(\lambda_h\left(\lambda_h\left(h_c(N) - h_r\right) + 4\dot{h}_c(N)\right)\right.\right. \\ \qquad \left.\left. +6\ddot{h}_c(N)\right) + 4\dddot{h}_c(N)\right) \\ h_c(N+1) = h_c(N) + \tau * \dot{h}_c(N) \\ \dot{h}_c(N+1) = \dot{h}_c(N) + \tau * \ddot{h}_c(N) \\ \ddot{h}_c(N+1) = \ddot{h}_c(N) + \tau * \dddot{h}_c(N) \\ \dddot{h}_c(N+1) = \dddot{h}_c(N) + \tau * fs_2(N) \end{cases} \quad (67)$$

where N is the number of iteration, λ_v and λ_h are the "velocity factors" which are related with the speed of the arranged transition process, and τ is the time step. Here, we choose λ_v=0.18, λ_h=0.18 and τ=0.01.

The parameters of our controller are given as follows: $k_{10} = 1, k_{11} = 3, k_{12} = 3, k_{20} = 81, k_{21} = 108, k_{22} = 54, k_{23} = 12, \gamma_1 = 12, \gamma_2 = 0.02, \boldsymbol{Q}_v = 200\boldsymbol{I}, \boldsymbol{Q}_h = \boldsymbol{I}, \sigma_v = 0.01, \sigma_h = 0.048,$ while the parameters of the nonlinear high gain observer are selected as: $\alpha_{v1} = 3, \alpha_{v2} = 3, \alpha_{v3} = 1, \alpha_{h1} = 4, \alpha_{h2} = 6, \alpha_{h3} = 4, \alpha_{h4} = 1, \varepsilon_v = 0.065, \varepsilon_h = 0.05.$ Besides, each of the antecedent fuzzy sets of our AIT2-FLS $\tilde{F}_1^s$ and $\tilde{F}_2^s$ has 5 MFs, namely NB, NS, ZO, PS and PB, with the parameter details shown in Table 1. The predefined consequent centroid vectors $\boldsymbol{\theta}_v^0$ and $\boldsymbol{\theta}_h^0$ as well as the initial values of

the adaptive parameter vectors $\boldsymbol{\theta}_v$ and $\boldsymbol{\theta}_h$ are set as the desired ones of the nominal model.

To verify the robustness of our proposed AIT2-FOFC scheme, additional uncertainties are added to the parameters in (7)-(10), with the drag D being 20% and the other three being -20%. The simulation results are displayed in Fig 3-Fig 6. From Fig 3 we can see that both the velocity and altitude present a good tracking performance in the face of unknown flexible dynamics and parameter uncertainties. Although there exist small tracking errors, Fig 4 still shows the effectiveness and convergence of our nonlinear high gain observer. Fig 5 depicts the control inputs of the system, including elevator deflection and throttle setting. We can see that in the transition process both the control inputs have a little vibrations due to the existence of large model uncertainties, while in the steady state process both become smooth and stable. At last, the outputs of the AIT2-FLS are shown in Fig 6, which demonstrates its strong capability of approximating uncertainties.

7 CONCLUSIONS

This paper mainly proposes an AIT2-FOFC scheme based on nonlinear high gain observer for FAHVs. After calculating the derivatives of the outputs repeatedly, we formulate the state feedback dynamic inversion controller as the basic controller. Besides, the AIT2-FLS is constructed to approximate the unknown model uncertainties, including flexible dynamics and parameter uncertainties. Moreover, the nonlinear high gain observer is applied to estimate the unmeasurable high order derivatives of the outputs. The overall output feedback control scheme is finally obtained based on the separation principle. Simulation conducted at last validates the effectiveness of our proposed method. In our future work, measurement noises will be taken into consideration, which leads to a further research on noise reduction property of our AIT2-FOFC scheme.

Table 1. Parameters of the Antecedent Fuzzy Sets

	$\underline{m}_{\tilde{F}_1^s}, \bar{m}_{\tilde{F}_1^s}$	$\underline{\sigma}_{\tilde{F}_1^s}$	$\bar{\sigma}_{\tilde{F}_1^s}$	$\underline{m}_{\tilde{F}_2^s}, \bar{m}_{\tilde{F}_2^s}$	$\underline{\sigma}_{\tilde{F}_2^s}$	$\bar{\sigma}_{\tilde{F}_2^s}$
NB	7846.4	18	32	0.0219	0.0012	0.0022
NS	7921.4	18	32	0.0270	0.0012	0.0022
ZO	7996.4	18	32	0.0322	0.0012	0.0022
PS	8071.4	18	32	0.0374	0.0012	0.0022
PB	8146.4	18	32	0.0426	0.0012	0.0022

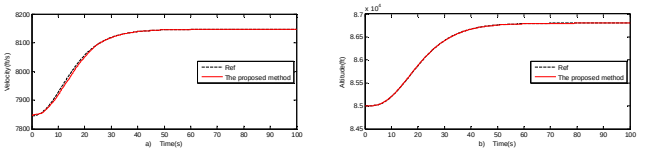

Fig 3. Velocity and altitude responses.

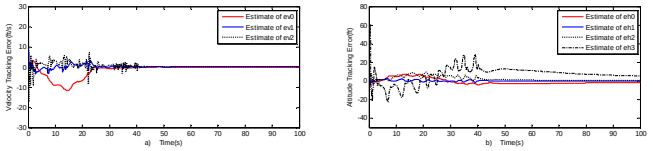

Fig 4. Outputs of nonlinear high gain observer.

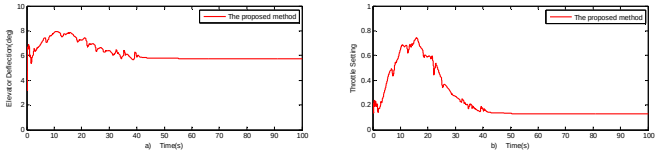

Fig 5. Control inputs.

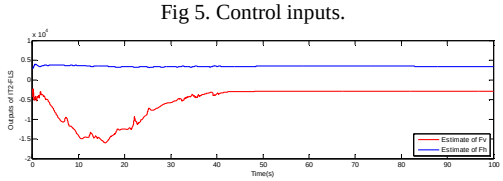

Fig 6. Outputs of AIT2-FLS.

REFERENCES

[1] M. A. Bolender and D. B. Doman, Nonlinear longitudinal dynamical model of an air-breathing hypersonic vehicle, Journal of Spacecraft and Rockets, vol. 44, pp. 374-387, 2007.

[2] H. J. Xu, M. D. Mirmirani, and P. A. Ioannou, Adaptive sliding mode control design for a hypersonic flight vehicle, Journal of Guidance, Control, and Dynamics, vol. 27, pp. 829-838, 2004.

[3] Z. Q. Pu, X. M. Tan, J. Q. Yi, and G. L. Fan, Advanced inversion control for a hypersonic vehicle based on PSO and arranged transient process, International Conference on Mechatronics and Automation, 359-364, 2011.

[4] X. D. Li, B. Xian, C. Diao, Y. P. Yu, K. Y. Yang, and Y. Zhang, Output feedback control of hypersonic vehicles based on neural network and high gain observer, Science China Information Sciences, vol. 54, pp. 429-447, 2011.

[5] J. J. He, R. Y. Qi, B. Jiang, and J. S. Qian, Adaptive output feedback fault-tolerant control design for hypersonic flight vehicles, Journal of the Franklin Institute, vol. 352, pp. 1811-1835, 2015.

[6] M. Wagenknecht and K. Hartmann, Application of fuzzy sets of type 2 to the solution of fuzzy equations systems, Fuzzy Sets and Systems, vol. 25, pp. 183-190, 1988.

[7] L. Fiorentini, A. Serrani, M. A. Bolender, and D. B. Doman, Nonlinear robust adaptive control of flexible air-breathing hypersonic vehicles, Journal of Guidance, Control, and Dynamics, vol. 32, pp. 402-417, 2009.

[8] M. A. Bolender and D. B. Doman, Flight path angle dynamics of air-breathing hypersonic vehicles, AIAA Paper 2006-6692, 2006.

[9] L. Fiorentini, Nonlinear adaptive controller design for air-breathing hypersonic vehicles, Ph.D dissertation, Electrical and Computer Engineering Department, The Ohio State University, 2010.

[10] J. M. Mendel, On KM algorithms for solving type-2 fuzzy set problems, IEEE Transactions on Fuzzy Systems, vol. 21, pp. 426-446, 2013.

[11] H. Ying, General interval type-2 Mamdani fuzzy systems are universal approximators, North American Fuzzy Information Processing Society Conference, 1-6, 2008.

[12] J. J. E. Slotine and W. P. Li, Applied Nonlinear Control. Prentice Hall NJ, 1991.

[13] H. K. Khalil, Nonlinear Systems, 3rd ed. Prentice Hall NJ, 2002.

[14] J. Q. Han, Active Disturbance Rejection Control Technique-the Technique for Estimating and Compensating the Uncertainties. National Defense Industry Press Beijing, China (in Chinese), 2008.